

# Impact of Transmission Data Characteristics on Quantitative Images for 4D PET

Yuzuru Kono<sup>1\*</sup>, Yasuhiro Wada<sup>2</sup>, Hiroaki Kurihira<sup>1</sup>, Hideaki Kitamura<sup>1</sup>, Daisuke Fujiyama<sup>1</sup>, Tomohiko Aso<sup>1</sup> and Masahiro Fukushi<sup>3</sup>

<sup>1</sup>Department of Radiology, National Cancer Center Hospital, Japan

<sup>2</sup>Molecular Probe Dynamics Laboratory, RIKEN Center for Molecular Imaging Science, Japan

<sup>3</sup>Radiological Sciences, Tokyo Metropolitan University, Japan

## Abstract

**Objective:** This study analyzed four-dimensional computed tomography (4DCT) imaging data characteristics and its impact on attenuation correction for 4D positron emission tomography (PET).

**Methods:** Four spheres of an International Electrotechnical Commission (IEC) Body Phantom Set<sup>TM</sup> were selected. Two <sup>18</sup>F concentrations (21.2 and 42.4 kBq/mL) with no surrounding activity were studied. The spheres moved to the cranial-caudal axis with 2 cm range. The cine CT scan parameters were as follows: 120 kVp, 10 mA, 5s, and full scan mode. CT reconstructed temporal sampling scales, directly reflecting spatial resolution in theory, were 0.33 s, 0.5 s, and 5 s. Emission data were acquired in 4D mode and the acquisition duration was 16 min in 8 phases. Attenuation-corrected PET data with those transmission datasets were compared and analyzed with each other.

Recovery coefficients (RCs) were calculated using the equation,  $RC=C_i/C_r$ , where  $C_i$  and  $C_r$  represent the maximal concentration of radioactivities in the VOI and in the fixed 37 mm sphere without motion, respectively. Several clinical examples comparing to static PET attenuated with "Average CT" (ACT) were included to illustrate its application.

**Results:** In the phantom PET study at 2.1 kBq/mL fluorodeoxyglucose (FDG) density, RC was  $0.77 \pm 0.11$  (partial-scan),  $0.58 \pm 0.06$  (full scan), and  $0.61 \pm 0.06$  (ACT). At 4.2 kBq/mL FDG density, RC was  $0.97 \pm 0.09$  (partial-scan),  $0.74 \pm 0.07$  (full scan), and  $0.56 \pm 0.04$  (ACT). In the patient study, SUV maximum values of the partial-scan reconstruction technique were higher than those of ACT PET by 2.8 to 22.6% (average  $\pm$  SD,  $11.5 \pm 6.6$ ). SUV average values were higher on 4DPET/CT with partial-scan reconstruction than those of ACT PET by 3.6 to 17.8% ( $12.6 \pm 5.7$ ).

**Conclusion:** Our findings suggest that attenuation correction with spatially detailed transmission data could be one way to secure 4DPET quantitative measurement.

**Keywords:** Attenuation correction; Motion artifacts; Temporal sampling; Spatial resolution

## Introduction

Cancer will soon become the most common cause of death worldwide. Among types of cancer, lung cancer is the predominant cause of cancer-related death. Of 203,536 individuals diagnosed with lung cancer during 2007 in the United States, 158,683 died as a direct result of the disease [1]. Use of fluorodeoxyglucose (FDG) positron emission tomography (PET) scanning is approved for Medicare reimbursement by the US Centers for Medicare and Medicaid Services (CMS) when performed for diagnosis, staging, and restaging of patients with lung cancer and/or suspicion of lung cancer. In general, standardized uptake value (SUV) is believed to be an indicator of tumor avidity and a predictor of patient survival rates [2]. However, general consensus maintains that SUV varies depending on many factors. For quantitative analysis, it is necessary to make corrections for dead time, delays, attenuation, scatter, physical half life, normalization applied to equalize the detector response and so on. Added to these, respiratory motion correction is essential near the diaphragm. We should notice that respiratory motion causes thoracic anatomy to change in all four dimensions (4D=3D space+time). And that the extent and speed of tumor motion varies widely among patients.

While CT diagnostic studies proceed while the patient holds his breath, spiral CT scanning under shallow free breathing is standard procedure for routine PET/CT studies. This is generally thought to

promote phase and spatial matching to those of PET; it requires long acquisition time in the order of several minutes. However, the two-dimensional (2D) nature of CT data acquisition and the interpolation process for reconstruction of transaxial data do not allow CT images of a moving object to represent a stationary object, nor do they include information on the total extent of the motion. Typical spiral CT acquisition results in poor reproduction of moving objects that cause motion artifacts known as smearing or blurring. Such CT artifacts should cause the quality of CT images and of measured attenuation correction to deteriorate.

Respiratory-gating systems for PET and PET/CT have been developed and tested to solve this problem. Presently the most sophisticated commercially available system is the Varian Real-time Position Management<sup>TM</sup> (RPM) system (Varian Medical Systems, Palo

**\*Corresponding author:** Yuzuru Kono, MS, Department of Radiology, National Cancer Center Hospital, 5-1-1 Tsukiji, Chuo-ku, Tokyo 104-0045, Japan, Tel: +81-03-3542-2511; Fax: +81-03-3542-3815; E-mail: [ykouno@ncc.go.jp](mailto:ykouno@ncc.go.jp)

Received June 19, 2012; Accepted July 02, 2012; Published July 05, 2012

**Citation:** Kono Y, Wada Y, Kurihira H, Kitamura H, Fujiyama D, et al. (2012) Impact of Transmission Data Characteristics on Quantitative Images for 4D PET. J Nucl Med Radiat Ther S3:005. doi:10.4172/2155-9619.S3-005

**Copyright:** © 2012 Kono Y, et al. This is an open-access article distributed under the terms of the Creative Commons Attribution License, which permits unrestricted use, distribution, and reproduction in any medium, provided the original author and source are credited.

Alto, CA, USA). In this system, CT data for attenuation correction are acquired in 4D mode [3]. A 4DCT scan is generated by acquiring CT projections over several respiratory cycles. The projections are resorted into several bins using an external motion monitor, based on the respiratory phase and a time series of 3D volume is generated. This series describes the motion of the volume over a single “representative” cycle.

Partial-scan CT providing optimized spatial resolution for moving targets has received only limited attention in the scientific literature and few investigators have addressed the challenge of its application in attenuation correction for PET, mainly due to increasing image noise. Partial-scan reconstruction algorithms uses data from one continuous  $240^\circ$  ( $180^\circ$ +fan angle) sweep of the x-ray tube for image reconstruction. Thus, the temporal resolution of these algorithms corresponds to approximately two-thirds of the gantry rotation time. Here, we analyzed the impact of this technique on 4D PET attenuation correction and investigated its applicability in clinical cases.

## Materials and Methods

### Phantom

The National Electrical Manufacturers Association (NEMA) 2001 International Electrotechnical Commission (IEC) phantom (Data Spectrum Corp., Hillsborough, NC, USA) composed of a quasi-cylindrical cavity ( $280 \times 210 \times 180$  mm) with fillable plastic spheres (Model ECT/IEC -BODY/P) was used. The inner diameters of the spheres were selected as 17, 22, 28, and 37 mm, considering the specifications of the PET scanner: a transaxial resolution of 5.1 mm at an axial resolution of 5.6 mm FWHM. Each sphere moved in air parallel to the cranial-caudal axis using a custom-designed electrical device (Figure 1) with no surrounding background activity. The  $^{18}\text{F}$  concentrations representing radioactive lesion activities were 21.2 and 42.4 kBq/mL [4].

### Patients

Nine patients (6 male, 3 female; average age, 68.7 y; age range, 62-78 y) with a biopsy-proven diagnosis of lung cancer, confirmed by staff pathologists at our institution, were included in this pilot prospective study. Patients were selected on the basis of clinical referral for evaluation of a documented or suspected primary or secondary malignancy in the lungs. Three patients presented  $^{18}\text{F}$  uptake lesions in

right lobe of S6, 2 left lobes in S8, 2 right lobes in S9, and 2 right lobes in S10.

### PET/CT Scanner

The Discovery 600 PET/CT scanner (GE Healthcare, Milwaukee, WI, USA) was used. PET images were reconstructed using a 3D ordered-subsets expectation-maximization (3D-OSEM) algorithm; 2 iterations, 16 subsets, and a post-filter of 5 mm (FWHM).

### Respiratory gating system

The RPM respiratory gating system has been applied to gated radiotherapy of the lung [5,6] respiratory-gated CT, and 4DCT, as well as to respiratory-gated PET imaging [3]. The system tracks the vertical displacement of two infrared reflective markers attached to a plastic box by an infrared video camera mounted on the PET/CT bed. RPM using 4DCT was originally investigated to improve target delineation in radiation therapy [7-9]. The conceptual basis for 4DCT is that images are oversampled at every position of interest along the long axis of the patient, and each image is tagged with breathing phase information. After the scan is completed, images are sorted based on the corresponding breathing phase signals. Many 3DCT sets are thus obtained, each corresponding to a particular breathing phase, and together they constitute a 4DCT set covering the entire breathing cycle. Thus, 4DCT decreases motion artifacts and accurately assesses the extent of intrafraction motion [10].

Motion trace was sampled at a rate of 30 Hz. The RPM system recorded amplitude, phase and time at each step, as well as the CT X-ray tube on/off times, and time-stamped each CT slice during the respiratory phase. **Average CT**

This method uses respiration-averaged CT (ACT) data obtained from 4D CT data sets. The advantage of using ACT is matching the temporal resolutions of the CT and static PET data [11]. Static PET data corrected with ACT were equally divided into eight frames of 2 min each (total 16 min) in this study.

### Partial scan CT

For motion-free imaging of the tumour, data have to be acquired during phases of the respiratory cycle with little tumour motion and with high temporal resolution. Sampling scale determines CT temporal resolution, which depends on gantry rotation time and further improvements can be achieved through partial scans:  $180^\circ$ + fan angle (e.g. 500 ms gantry rotation time=330 ms temporal resolution). Temporal, spatial and contrast resolution are to be optimized and also radiation exposure to the patients to be limited in this way. Note that this technique can also be applicable to the scanners from other vendors.

### 4D PET/CT acquisition of phantom

As sensitivity is not uniform across the field of view of the PET scanner, the phantom was carefully positioned in the center of the axial part of the scan field of view to achieve consistent stable resolution. The longitudinal peak-to-peak amplitude settings were 2 cm and the frequency of motion was set to approximately one rotation every four seconds. Emission data were acquired using RPM respiratory gating system in 4D mode with  $192 \times 192$  reconstruction matrices ( $3.65 \times 3.65 \times 2.18$  mm). The acquisition duration was 16 min in 8 phase gated mode; temporal resolution of PET data was 0.5 s (one motion cycle of 4s/8gate phases). Then 4DCT was performed and scan parameters for the system were as follows: 120 kVp, 10 mA, full scan



**Figure 1:** Phantom setup for Discovery 600™ with moving spheres. Custom-designed electronic device enables spheres to move parallel to cranial-caudal axis.

mode, X-ray collimation of 8×2.5 mm, gantry rotation cycle of 0.5 s, and slice thickness of 2.5 mm. Temporal resolution or “scan data duration” of reconstructed CT imaging were, 0.33 s (partial-scan reconstruction), 0.5 s (full scan reconstruction), and 5 s (ACT). Cine CT duration was fixed at 5s to ensure cine CT data of more than one motion. The total scan length was set to cover full displacement of the target.

### PET/CT Acquisition of Patients

Patients were fasted for at least 4 h before injection of 180-272.8 MBq of <sup>18</sup>F-FDG depending on their weights. Patients were trained to repeat a constant breathing pattern (“breathe in, breathe out”), which aimed to ensure that the RPM system would function properly before the injection.

Clinical PET/CT protocols are follows as: a scout image with settings of 120 kV and 10 mA was first acquired to determine the scanning field of the patient. This was followed by 16-slice helical CT scanning using the following scanning parameters: gantry rotation, 0.5 s/rotation, 120 kV and 150 mA; matrix, 512×512; slice thickness, 2.5 mm; pitch, 1.75; beam collimation, 20 mm. This scan was then followed by a whole-body PET scan approximately 60 min after injection in three-dimensional (3D) mode, so that it covered the same area with 2 min per bed position. These CT and PET scans were acquired under free shallow breathing with no voice instructions.

After the clinical PET/CT, patients remained in the same position (supine, hands down), and a plastic box with 2 infrared reflective markers were placed on the abdomen for respiratory motion tracking. The RPM respiratory gating system in amplitude-gating mode was used to monitor and track the patient’s respiratory motion. Emission data were acquired utilizing RPM after 90 min interval of FDG injection in 4D mode with 192×192 reconstruction matrices (3.65×3.65×2.18 mm). The acquisition duration was 16 min in 8 phase gated mode. 4DCT was then performed and scan duration was increased to ensure cine CT data of more than one respiratory cycle. Note that CT data were acquired in partial-scan mode based on our phantom study results. Our institution routinely adds 1 s to a breathing cycle. The total scan length was set to cover full displacement of the target.

We compared the 3D-static PET data attenuated with ACT to 4DPET attenuated with partial-scan 4DCT. This study protocol was approved by the institutional review board and written informed consent was obtained.

### Data analysis

Data were analyzed using Advantage Workstation Volume Share™ 2 (GE Healthcare, Chalfont St. Giles, UK). Threshold values were set in the analysis for objectivity and reproducibility in phantom studies. The sphere volumes in CT images were determined by setting maximum and minimum thresholds at 100 and -100 HU, respectively. Ratio of displaced volume was calculated to analyze the effects of motion amplitude and object size [12]. Note that the values were calculated from the equation: maximum sphere displacement/sphere diameter×100 (%). For PET volume analysis; threshold values for the moving and fixed phantoms were set at 36%. The value was determined from the phantom experiments with reference to published data [13,14]. The volumes of the spheres calculated by the software and the actual volumes were compared.

The recovery coefficient (RC) was calculated to quantitatively evaluate the PET data using the equation, RC=Ci/Cr, where Ci and Cr represent the maximal concentration of radioactivity in the volume of

interest and in the fixed 37 mm sphere without motion, respectively. The reference for each parameter was the maximal concentration of radioactivity in the 37 mm fixed sphere.

In the clinical study, 4DPET/partial-scan reconstruction CT and static PET/ACT were examined. Maximum (SUV max) and average SUV values and lesion volume were manually defined with the adaptive thresholding method by an experienced physician [13]. Both SUV max and average SUV were normalized to body weight. Images were also visually assessed for accuracy of fusion and alignment. Data were statistically analyzed using the Tukey HSD and multivariate Student’s t-test (SPSS Inc., Chicago, IL, USA). The level of significance was set at p<0.05.

## Results

### Phantom study

Table 1 shows a comparison of average HU of the sphere images among three different reconstruction techniques. No significant differences were observed. HU of partial-scan was 0.8 ± 1.6, that of full scan was -0.7 ± 1.4, and that of average CT was -6.3 ± 2.9. True HU of the spheres was zero.

Table 2 compares the impact of the different reconstruction strategies on CT image noise using the static phantom. The noise was reduced by one third between partial-scan reconstruction and Average CT. On the contrary, no significant difference was observed between partial-scan and full scan reconstruction.

Figure 2 shows an example of CT images of those techniques (window width: 1000 HU, window level: 0 HU).

Table 3 summarizes RCs and volume percentage errors of PET data among the techniques. Partial-scan reconstruction technique had statistically less count loss than those of the other techniques (P<0.05). Note that (n=64) in the Tables stands for two <sup>18</sup>F radioactive lesion activities of four spheres gating in eight phases and that (n=8) stands for two <sup>18</sup>F radioactive lesion activities of four spheres. For PET data

Ratio of displaced	Partial-scan (n=64)	Full scan (n=64)	Average CT (n=8)
Volume (%)*	HU	HU	HU
54.1	-0.6	-2.3	-3
71.4	-0.1	-1.2	-6
90.9	1	0.5	-6
117.6	2.9	0.4	-10
Mean ± SD	0.8 ± 1.6	-0.7 ± 1.4	-6.3 ± 2.9

\*Ratio of displaced volume = maximum sphere displacement/sphere diameter×100 (%). True HU is 0

**Abbreviations:** HU=Hounsfield units, CT=computed tomography  
Note that (n=64) in the tables stands for two <sup>18</sup>F radioactive lesion activities of four spheres gating in eight phases and that (n=8) stands for two <sup>18</sup>F radioactive lesion activities of four spheres

**Table 1:** Comparison of average Hounsfield units (HU) in computed tomography (CT) images acquired by different reconstruction techniques.

	Partial-scan reconstruction	Full scan reconstruction	Average CT reconstruction
CT noise	9.2	7.2	3.0

Date represent Standard Deviation (SD) within a ROI setup calculated in CT images of each reconstruction technique  
Image noise is related to CT temporal sampling scale: partial-scan reconstruction (0.33 s), full scans reconstruction (0.5 s), and average CT reconstruction (5 s)

**Table 2:** The impact of the different CT reconstruction strategies on noise in CT images.

at 2.1 kBq/mL FDG density, RC ranged from 0.63 to 1.00 ( $0.77 \pm 0.11$ ) (partial-scan), from 0.49 to 0.67 ( $0.58 \pm 0.06$ ) (full scan), and from 0.52 to 0.70 ( $0.61 \pm 0.06$ ) (ACT). Volume error ratio (%) ranged from -10.5 to 12.5 ( $2.6 \pm 1.4$ ) (partial-scan), from -11.0 to 7.5 ( $-1.0 \pm 3.3$ ) (full-scan), and from -17.6 to 7.1 ( $-3.1 \pm 1.6$ ) (ACT). At 4.2 kBq/mL FDG density, RC ranged from 0.83 to 1.12 ( $0.97 \pm 0.09$ ) (partial-scan), from 0.63 to 0.86 ( $0.74 \pm 0.07$ ) (full scan), and from 0.52 to 0.63 ( $0.56 \pm 0.04$ ) (ACT). Volume error ratio (%) ranged from -14.4 to 20.2 ( $2.1 \pm 2.1$ ) (partial-scan), from -16.2 to 32.7 ( $9.6 \pm 1.8$ ) (full-scan), and from

-15.2 to 0.7 ( $-5.0 \pm 2.5$ ) (ACT). These data suggest that partial-scan reconstruction CT data is effective in improving data from 4DPET scanning of moving objects.

### Patient study

Figure 3 displays examples of CT (window width: 400, window level: 40), their histograms of HU and fusion images (bottom SUV: 0, top SUV: 6). Clinical CT histogram showed a sharper peak: soft tissue (19HU) than the other techniques. The size of all lesions, detected on

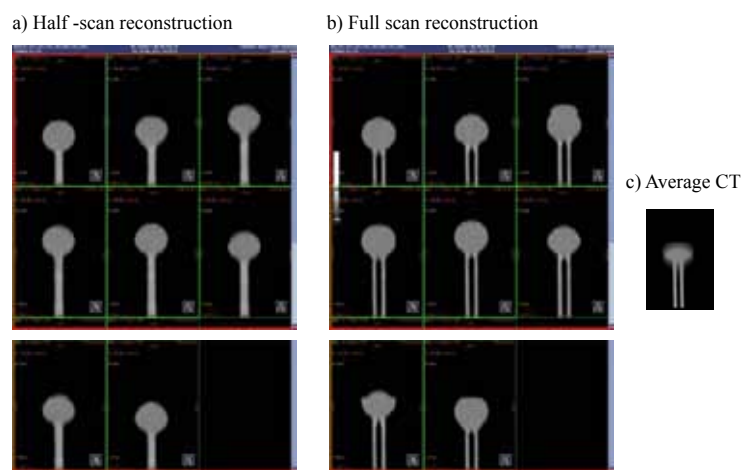


**Figure 2:** Comparison of partial-scan, full scan, and average CT reconstruction image of cine CT data. Although having better high-contrast resolution and better edge definition, partial-scan reconstruction images have more noise.

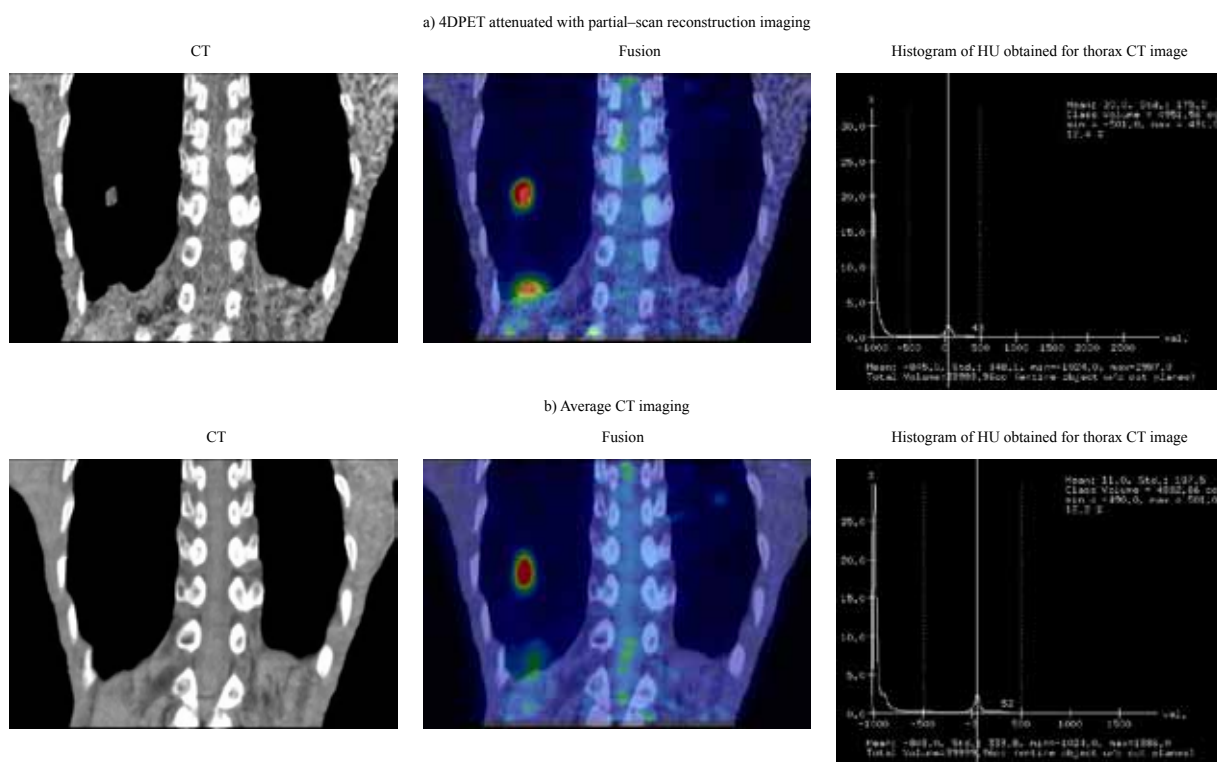


**Figure 3:** Clinical images and HU histograms of different CT reconstruction images. Each image was constructed on the SUV max point level. 4DPET with partial-scan reconstruction imaging succeeded in reducing misalignment to a minimum level. Each reconstruction histogram was able to distinguish two distinct peaks: air (-1000 HU) and soft tissue (30: partial scan, 11: ACT, and 19: Clinical PET/CT).

clinical CT with breath held performed within 7 days of the PET/CT studies, ranged from 1.2 cm to 5.8 cm ( $3.0 \pm 1.7$  cm).

SUV max, SUV average, and contoured volume with the three techniques are shown in Table 4. SUV max values were higher with 4DPET/CT with partial-scan reconstruction than with ACT PET by 2.8 to 22.6% ( $11.5 \pm 6.6$ ). Average SUV values were higher with 4DPET/CT with partial-scan reconstruction than with ACT PET by 3.6 to 17.8% ( $12.6 \pm 5.7$ ). Contoured volumes were smaller with 4DPET/CT with partial-scan reconstruction than with ACT PET by 2.8 to 36.8% ( $12.6 \pm 9.7$ ). SUV max values were higher on 4DPET/CT with partial-scan reconstruction than with clinical PET by 10.1 to 52.7% ( $25.9 \pm 15.3$ ). Average SUV values were higher with 4DPET/CT with partial-scan reconstruction than with clinical PET by 5.5 to 54.5% ( $28.5 \pm 16.4$ ). Contoured volumes were smaller with 4DPET/CT with partial-scan reconstruction than with clinical PET by 1.1 to 33.9% ( $15.0 \pm 16.5$ ).

## Discussion

Our moving phantom study suggested that attenuation correction value improve with transmission data of spatial accuracy. The patients' study suggested applicability of the 4DPET/CT in partial-scan mode

and resulted in increasing SUVs and decreasing calculated volume comparing to those of ACT. These results should conjecture that characteristics of transmission scan data effects greatly on quantitative PET images. The increased SUVs have significant meanings for surgically managed lung cancer patients, as being reported that the addition of SUV max to pathological tumour size identifies patients at highest risk as a result of recurrent disease after resection [15].

Respiratory motion causes two major phenomena in the diaphragm region; blurring of the image and attenuation correction errors. Forcing CT projection data acquired over several cycles into a few respiratory phase bins can lead to severe motion artifacts. Yamamoto et al. found that 45 of 50 patients had at least one, with a mean magnitude of 11.6 mm (range: 4.4-56.0 mm) [16]. One may argue that experienced PET readers can account for artifacts, but in some cases this misalignment can pose a serious diagnostic problem [17-19]. Attenuation correction is important because PET imaging is based on detecting the coincidence annihilation photon pair that must collectively travel the full width of the body, which produces a significant amount of attenuation. In the chest, lung tissue has a complex mixture of tissue and attenuation correction is considerably different from subject to subject, depends on

FDG concentration 2.1 kBq/mL						
	Partial-scan reconstruction		Full scan reconstruction		Average CT	
Sphere diameter : 17-mm	Mean $\pm$ SD	Range	Mean $\pm$ SD	Range	Mean $\pm$ SD	Range
RC	0.66 $\pm$ 0.03	0.63,0.71	0.51 $\pm$ 0.01	0.49,0.53	0.54 $\pm$ 0.01	0.52,0.56
Volume error (%)	4.3 $\pm$ 12.4	-14.4, 20.2	-1.3 $\pm$ 5.6	-10.5, 6.6	-4.1 $\pm$ 6.1	-11.3, 4.3
Sphere diameter : 22-mm						
RC	0.71 $\pm$ 0.04	0.63,0.76	0.56 $\pm$ 0.02	0.53,0.59	0.59 $\pm$ 0.01	0.57,0.61
Volume error (%)	1.8 $\pm$ 6.4	-7.7, 10.2	2.2 $\pm$ 4.6	-5.0,7.5	-2.1 $\pm$ 8.1	-17.6, 0.4
Sphere diameter : 28-mm						
RC	0.81 $\pm$ 0.05	0.80,0.86	0.60 $\pm$ 0.02	0.60,0.61	0.64 $\pm$ 0.01	0.62,0.67
Volume error (%)	1.2 $\pm$ 7.6	-10.5, 10.7	-5.5 $\pm$ 4.4	-11.0, 2.1	-4.7 $\pm$ 4.1	-10.4, 0.8
Sphere diameter : 37-mm						
RC	0.94 $\pm$ 0.04	0.90,1.00	0.64 $\pm$ 0.03	0.61,0.67	0.67 $\pm$ 0.01	0.66,0.70
Volume error (%)	3.2 $\pm$ 5.5	-5.9, 10.1	-2.1 $\pm$ 3.5	-7.6,3.1	-1.4 $\pm$ 3.7	-7.8, 2.3
FDG concentration 4.2 kBq/mL						
	Partial-scan reconstruction		Full scan reconstruction		Average CT	
Sphere diameter: 17-mm	Mean $\pm$ SD	Range	Mean $\pm$ SD	Range	Mean $\pm$ SD	Range
RC	0.86 $\pm$ 0.02	0.83, 0.90	0.67 $\pm$ 0.02	0.63, 0.69	0.52 $\pm$ 0.01	0.51,0.54
Volume error (%)	2.3 $\pm$ 7.1	-10.5, 12.5	11.7 $\pm$ 9.8	-3.8, 26.5	-6.6 $\pm$ 4.2	-14.4, -5.1
Sphere diameter : 22-mm						
RC	0.94 $\pm$ 0.02	0.92, 0.97	0.69 $\pm$ 0.01	0.67, 0.71	0.54 $\pm$ 0.01	0.52,0.55
Volume error (%)	4.9 $\pm$ 5.8	-5.0, 12.0	10.4 $\pm$ 16.7	-16.2, 32.7	-2.1 $\pm$ 4.9	-8.1, 4.3
Sphere diameter : 28mm						
RC	1.00 $\pm$ 0.02	0.97, 1.02	0.75 $\pm$ 0.02	0.73, 0.77	0.58 $\pm$ 0.01	0.56,0.59
Volume error (%)	-0.2 $\pm$ 5.3	-8.8, 7.2	8.0 $\pm$ 9.0	-4.0, 19.5	-7.5 $\pm$ 4.5	-15.2, -2.2
Sphere diameter : 37-mm						
RC	1.06 $\pm$ 0.03	1.01, 1.11	0.83 $\pm$ 0.02	0.81,0.86	0.61 $\pm$ 0.01	0.60, 0.63
Volume error (%)	1.2 $\pm$ 3.8	-5.0, 6.3	8.2 $\pm$ 14.6	-10.1, 31.0	-3.8 $\pm$ 3.9	-9.7, 0.7

\* RC=Ci/Cr $\times$ 100, where Ci and Cr represent the maximal concentration of radioactivity in the volume of interest and in the fixed 37 mm sphere without motion, respectively. Maximum radioactivity concentration of the 37-mm fixed sphere served as reference for each parameter

**Table 3:** Comparison of recovery coefficients (RC) and calculated volume errors of four-dimensional positron emission tomography (4DPET) images with different computed tomography (CT) attenuation correction.

No		Partial-scan reconstruction CT (n=8)	Average CT (n=8)	P	Clinical PET/CT
1	SUV max	9.7 ± 0.4	9.0 ± 0.5	0.009*	8.6
	SUV average	5.9 ± 0.2	5.1 ± 0.3	<0.001*	5
	Calculated volume (mL)	3.8 ± 0.1	4.2 ± 0.2	0.001*	3.8
2	SUV max	3.9 ± 0.4	3.1 ± 0.2	<0.001*	2.8
	SUV average	1.9 ± 0.2	1.5 ± 0.1	<0.001*	1.4
	Calculated volume (mL)	3.7 ± 0.8	5.6 ± 1.0	<0.001*	5.7
3	SUV max	12.3 ± 0.8	10.9 ± 0.5	<0.001*	9.8
	SUV average	7.3 ± 0.8	6.4 ± 0.3	0.007*	5
	Calculated volume (mL)	7.5 ± 0.5	8.3 ± 0.4	0.002*	8.0
4	SUV max	14.9 ± 0.4	14.5 ± 0.4	0.03*	12.2
	SUV average	8.8 ± 0.1	8.5 ± 0.2	0.001*	7.0
	Calculated volume (mL)	70.7 ± 1.7	72.7 ± 0.9	0.01*	74.8
5	SUV max	11.6 ± 1.3	10.8 ± 0.4	0.12	10.5
	SUV average	5.8 ± 0.3	5.5 ± 0.2	0.02*	5.1
	Calculated volume (mL)	163.1 ± 27.5	191.8 ± 11.9	0.02*	165.0
6	SUV max	5.3 ± 0.8	4.5 ± 0.2	0.03*	4.8
	SUV average	2.9 ± 0.5	2.4 ± 0.2	0.05*	2.7
	Calculated volume (mL)	13.2 ± 2.4	16.3 ± 1.3	0.02*	14.3
7	SUV max	9.7 ± 0.5	8.9 ± 0.6	0.01*	7.1
	SUV average	5.0 ± 0.3	4.6 ± 0.3	0.04*	3.9
	Calculated volume (mL)	11.0 ± 1.1	12.3 ± 0.9	0.05*	13.6
8	SUV max	14.0 ± 0.6	12.5 ± 0.5	<0.001*	12.5
	SUV average	8.0 ± 0.3	7.1 ± 0.3	<0.001*	6.9
	Calculated volume (mL)	3.1 ± 0.2	3.7 ± 0.2	0.11	3.9
9	SUV max	10.8 ± 0.8	8.3 ± 0.4	<0.001*	7.6
	SUV average	5.9 ± 0.4	4.6 ± 0.3	<0.001*	3.7
	Calculated volume (mL)	1.5 ± 0.2	2.2 ± 0.3	<0.001*	3.7

\* indicates statistically significant

Data represent the mean ± SD

Acquisition duration of partial scan reconstruction and average CT was 16 min in 8 phase gated mode respectively. Emission data were acquired utilizing RPM after 90 min interval of FDG injection

Acquisition duration of clinical PET/CT was 2 min/bed. Emission data were acquired after 60 min interval of FDG injection under free shallow breathing with no voice instructions

**Table 4:** Behavior of standardized uptake value and calculated volume with the three techniques.

breathing patterns, and varieties with age and in the event of respiratory diseases by as much as 30% [20]. What makes things more complicated is that attenuation correction errors are mainly caused due to the shadow of the patients' diaphragm rather than to the tumor motion [4]. We should often notice that the simple application of phase matching between PET and CT cannot improve the attenuation correction.

Traditional transmission scans with <sup>68</sup>Ge-<sup>68</sup>Ga sources can match emission scans in terms of temporal resolution to the extent that patients can remain immobile throughout a long acquisition period. One major limitation of this technique is statistical fluctuations due to a limited amount of radioactivity and to attenuation correction factors taken as the ratio between blank and transmission sinograms. The transmission source is very close to the detector ring, so the nearby detector is constantly exposed to intensive  $\gamma$ -rays. Moreover, newer PET/CT scanners are not equipped with transmission sources.

Several approaches have been advocated to improve the accuracy of attenuation correction in PET/CT. One is to slow the CT gantry rotation (for example, 4 s/ rotation) to obtain an average CT scan to match the PET data, but this can produce streaking artifacts in images [21].

ACT, which in a sense is a sophisticated slow CT technique, has been validated by a large number of clinical cases [4]. The advantages of this technique include a marked reduction in total examination time. And that it should be applicable in cases of variable breathing patterns

during data acquisition. We may say that the interpreting physician should select the specific protocol between ACT and 4D PET/CT to be performed after carefully monitoring patients' respiration.

A few drawbacks might be associated with using partial-scan reconstruction. One is larger data volume, but constant improvements in computing power and data storage should address this. Another might be increased noise in CT images. Statistical noise in the transmission measurements can increase significantly the noise level in the reconstructed emission images. However, in the way of smoothing of the transmission sinograms reducing statistical fluctuations and converting CT images to 511-keV attenuation maps to form sinograms of PET attenuation factors resulted in no adverse effects but improved PET data. We need mention here only that in the low-dose CT both x-ray beam energy and beam current are set as low as reasonably possible to minimize radiation exposure to the patient, which will result in having high statistical image noise by itself. If adopted in PETCT scanners, newer Dual-source CT, which yields high true temporal resolution, may be promising. What should also be mentioned is that partial-scan reconstruction technique will need to be adjusted for patient size and the tumor location not to cause a discrepancy in the pixel values. Larger patients have streak artifacts from beam-hardening artifacts. The scan target should be sufficiently centered within the scan field of view in order to maintain a consistent and stable temporal resolution.

Some may argue that it would make sense to match the 4DCT scan reconstruction with the gated PET temporal resolution to drive a more

consistent reconstruction. However, to obtain high spatial and contrast resolution CT data should be given higher priority for quantitation according to our phantom study.

One of the limitations to be solved for 4DCT is its radiation dose. The reported radiation dose is 5 mGy for ACT based on a 10 mA cine CT scan of 5.9 s duration, and approximately 1.35 mSv for an effective radiation dose of 10 mA for ACT covering 16 cm of the thorax [22]. This dose may not be a critical issue in radiation therapy planning. However, for serial studies, paediatric studies, this dose should be rather high. This report also suggests that partial-scan acquisition should address this. Radiation dose could be reduced by 33% comparing to full-scan acquisition.

Although ours was a preliminary study and further studies are needed, in our opinion, attenuation correction with partial-scan CT data is one way to create quantitative 4D PET images.

### Study limitation

In the experimental phantom study, analysis was conducted only in the center of the axial part of the scan field of view with high sensitivity. Reduced sensitivity area, at the ends of FOV, was not dealt with and continuing study should be warranted. In patient study, 4DCT was performed in partial-scan mode and we did not investigate cases of full scan owing to our phantom study results. Despite these limitations, our study is the first report to describe the application of partial scan reconstructed CT data for 4DPET attenuation correction and to demonstrate its validity.

### Conclusions

To create quantitative 4D PET images, they must be corrected for dead time, delays, attenuation, scatter, physical half life and normalization to equalize the detector response. For small structures around the diaphragm, corrections for partial volume, spill-over, and motion correction should also be needed. Absolute quantitation is challenging, therefore it may be practical to decide what level of quantitation be achieved. Our data suggested the validity of 4DPET corrected with partial-scan cine CT to meet the requirement.

### Acknowledgments

This study was supported in part by the Japanese Cancer Research Foundation.

### References

1. U.S. Cancer Statistics Working Group. United States Cancer Statistics: 1999–2007 Incidence and Mortality Web-based Report, USA.
2. Ahuja V, Coleman RE, Herndon J, Patz EF Jr. (1998) The prognostic significance of fluorodeoxyglucose positron emission tomography imaging for patients with nonsmall cell lung carcinoma. *Cancer* 83: 918-924.
3. Pan T, Sun X, Luo D (2007) Improvement of the cine-CT based 4D-CT imaging. *Med Phys* 34: 4499-4503.
4. National Electrical Manufacturers Association (NEMA) (2007) Performance Measurements of Positron Emission Tomographs (PETs). Rosslyn: NEMA standards publication NU2-2007.
5. Korreman SS, Juhler-Nottup T, Boyer AL (2008) Respiratory gated beam delivery cannot facilitate margin reduction, unless combined with respiratory correlated image guidance. *Radiother Oncol* 86: 61-68.
6. Ahmed RS, Shen S, Ove R, Duan J, Fiveash JB, et al. (2007) Intensity modulation with respiratory gating for radiotherapy of the pleural space. *Med Dosim* 32: 16-22.
7. Sarrut D, Boldea V, Miguet S, Ginestet C (2005) Simulation of 4D CT images from deformable registration between inhale and exhale breath-hold CT scans. *Int J Radiant Oncol Biol Phys* 63: S509-S510.

8. Low DA, Nystrom M, Kalinin E, Parikh P, Dempsey JF, et al. (2003) A method for the reconstruction of four-dimensional synchronized CT scans acquired during free breathing. *Med Phys* 30: 1254-1263.
9. Britton KR, Starkschall G, Tucker SL, Pan T, Nelson C, et al. (2007) Assessment of gross tumor volume registration and motion changes during radiotherapy for non-small-cell lung cancer as measured by four-dimensional computed tomography. *Int J Radiat Oncol Biol Phys* 68: 1036-1046.
10. Lagerwaard FJ, Van Sornsen de Koste JR, Nissen-Visser MR, Schuchhard-Schipper RH, Oei SS, et al. (2001) Multiple "slow" CT scans for incorporating lung tumor mobility in radiotherapy planning. *Int J Radiant Oncol Biol Phys* 51: 932-937.
11. Pan T, Mawlawi O, Nehmeh SA, Erdi YE, Luo D, et al. (2005) Attenuation correction of PET images with respiration-averaged CT images in PET/CT. *J Nucl Med* 46: 1481-1487.
12. Erdi YE, Nehmeh SA, Pan T, Pevsner A, Rosenzweig KE, et al. (2004) The CT motion quantitation of lung lesions and its impact on PET-measured SUVs. *J Nucl Med* 45: 1287-1292.
13. Erdi YE, Mawlawi EO, Larson SM, Imbriaco M, Yeung H, et al. (1997) Segmentation of lung lesion volume by adaptive positron tomography image thresholding. *Cancer* 80: 2505-2509.
14. Daisen JF, Sibomana M, Bol A, Doumont T, Lonnew M, et al. (2003) Tri-dimensional automatic segmentation of PET volumes based on measured source-to-background ratios: influence of reconstruction algorithms. *Radiother Oncol* 69: 247-250.
15. Downey RJ, Akhurst T, Gonen M, Vincent A, Bains MS, et al. (2004) Preoperative F-18 fluorodeoxyglucose-positron emission tomography maximal standardized uptake value predicts survival after lung cancer resection. *J Clin Oncol* 22: 3255-3260.
16. Yamamoto T, Langner U, Loo BW Jr, Shen J, Keall PJ (2008) Retrospective analysis of artifacts in four-dimensional CT images of 50 abdominal and thoracic radiotherapy patients. *Int J Radiant Oncol Biol Phys* 72: 1250-1258.
17. Sarikaya I, Yeung HW, Edri Y, Larson SM (2003) Respiratory artefact causing malpositioning of liver dome lesion in right lower lung. *Clin Nucl Med* 28: 943-944.
18. Erdi YE, Nehmeh SA, Pan T, Pevsner A, Rosenzweig KE, et al. (2004) The CT motion quantitation of lung lesions and its impact on PET-measured SUVs. *J Nucl Med* 45: 1287-1292.
19. Osman MM, Cohade C, Nakamoto Y, Marshall LT, Leal JP, et al. (2003) Clinically significant inaccurate localization of lesions with PET/CT: frequency in 300 patients. *J Nucl Med* 44: 240-243.
20. Robinson PJ, Kreef L (1979) Pulmonary tissue attenuation with computed tomography: comparison of inspiration and expiration scans. *J Comput Assist Tomogr* 3: 740-748.
21. Lagerwaard FJ, Van Sornsen de Koste JR, Nijssen-Visser MR, Schuchhard-Schipper RH, Oei SS, et al. (2001) Multiple "slow" CT scans for incorporating lung tumor mobility in radiotherapy planning. *Int J Radiant Oncol Biol Phys* 51: 932-937.
22. Pan T, Mawlawi O, Luo D, Liu HH, Chi PC, et al. (2006) Attenuation correction of PET cardiac data with low-dose average CT in PET/CT. *Med Phys* 33: 3931-3938.